NASA/TM-20220012622

Highlights of Aeroacoustic Tests of a Metal Spacecraft Cabin Ventilation Fan Prototype

David Stephens, Jonathan M. Goodman, Rebecca A. Buehrle, Arman Mirhashemi, L. Danielle Koch, Tony D. Shook, and Daniel L. Sutliff
Glenn Research Center, Cleveland, Ohio

Christopher S. Allen and Christopher M. Matty
Johnson Space Center, Houston, Texas

November 2022

NASA STI Program . . . in Profile

Since its founding, NASA has been dedicated to the advancement of aeronautics and space science. The NASA Scientific and Technical Information (STI) Program plays a key part in helping NASA maintain this important role.

The NASA STI Program operates under the auspices of the Agency Chief Information Officer. It collects, organizes, provides for archiving, and disseminates NASA's STI. The NASA STI Program provides access to the NASA Technical Report Server—Registered (NTRS Reg) and NASA Technical Report Server—Public (NTRS) thus providing one of the largest collections of aeronautical and space science STI in the world. Results are published in both non-NASA channels and by NASA in the NASA STI Report Series, which includes the following report types:

- TECHNICAL PUBLICATION. Reports of completed research or a major significant phase of research that present the results of NASA programs and include extensive data or theoretical analysis. Includes compilations of significant scientific and technical data and information deemed to be of continuing reference value. NASA counter-part of peer-reviewed formal professional papers, but has less stringent limitations on manuscript length and extent of graphic presentations.

- TECHNICAL MEMORANDUM. Scientific and technical findings that are preliminary or of specialized interest, e.g., "quick-release" reports, working papers, and bibliographies that contain minimal annotation. Does not contain extensive analysis.

- CONTRACTOR REPORT. Scientific and technical findings by NASA-sponsored contractors and grantees.

- CONFERENCE PUBLICATION. Collected papers from scientific and technical conferences, symposia, seminars, or other meetings sponsored or co-sponsored by NASA.

- SPECIAL PUBLICATION. Scientific, technical, or historical information from NASA programs, projects, and missions, often concerned with subjects having substantial public interest.

- TECHNICAL TRANSLATION. English-language translations of foreign scientific and technical material pertinent to NASA's mission.

For more information about the NASA STI program, see the following:

- Access the NASA STI program home page at http://www.sti.nasa.gov

- E-mail your question to help@sti.nasa.gov

- Fax your question to the NASA STI Information Desk at 757-864-6500

- Telephone the NASA STI Information Desk at 757-864-9658

- Write to:
  NASA STI Program
  Mail Stop 148
  NASA Langley Research Center
  Hampton, VA 23681-2199

NASA/TM-20220012622

Highlights of Aeroacoustic Tests of a Metal Spacecraft Cabin Ventilation Fan Prototype

David Stephens, Jonathan M. Goodman, Rebecca A. Buehrle, Arman Mirhashemi, L. Danielle Koch, Tony D. Shook, and Daniel L. Sutliff
Glenn Research Center, Cleveland, Ohio

Christopher S. Allen and Christopher M. Matty
Johnson Space Center, Houston, Texas

Prepared for the
Noise-Con 2022
sponsored by the Institute of Noise Control Engineering of the USA
Lexington, Kentucky, June 13–15, 2022

National Aeronautics and
Space Administration

Glenn Research Center
Cleveland, Ohio 44135

November 2022

Acknowledgments

This work was supported by NASA's Advanced Exploration Systems International Space Station Habitation, Environmental Control and Life Support System. The research team would like to thank Lenny Smith and Bruce Groene, T-FOME, for their help assembling the duct rig. We are also grateful for the photographs taken by Bridget Caswell, Jef Janis, and Mark Grills and the illustrations drawn by Terrence Condrich from NASA Glenn Research Center's Logistics and Technical Information Division.

Level of Review: This material has been technically reviewed by technical management.

This report is available in electronic form at http://www.sti.nasa.gov/ and http://ntrs.nasa.gov/

Highlights of Aeroacoustic Tests of a Metal Spacecraft Cabin Ventilation Fan Prototype

David Stephens, Jonathan M. Goodman, Rebecca A. Buehrle, Arman Mirhashemi,
L. Danielle Koch, Tony D. Shook, and Daniel L. Sutliff
National Aeronautics and Space Administration
Glenn Research Center
Cleveland, Ohio 44135

Christopher S. Allen and Christopher M. Matty
National Aeronautics and Space Administration
Johnson Space Center
Houston, Texas 77058

Abstract

A metal spacecraft cabin ventilation fan suitable for aerodynamic and acoustic ground tests was designed and tested in the NASA Glenn Research Center Acoustical Testing Laboratory. The fan design featured a low-noise blade-vane count that was chosen to reduce the rotor-stator interaction tone noise. The fan was throttled through its operating range, and results indicated that the measured aerodynamic and acoustic performance was in good agreement with predictions. Recommendations for further research of quiet high-performance fans intended to support long duration human space exploration missions are offered. This small fan aerodynamic and acoustic test rig and the NASA Glenn Acoustical Testing Laboratory are valuable resources available for supporting NASA's aeronautics research and space exploration missions. The computer-aided design (CAD) files used to manufacture the fan described in this report are available as a supplemental file (TM-20220012622-SUPPL1.pdf). The supplemental file contains the coordinates of the fan rotor, stator, and hub and tip endwalls (TM-20220012622-SUPPL2.zip), the solid model of the spacecraft cabin vent fan generated with CREO (TM-20220012622-SUPPL3.zip), and dimensioned two-dimensional drawings of the fan in *.pdf format (TM-20220012622-SUPPL4.zip).

1.0 Introduction

People need clean air to breathe and a quiet place to work, whether they are living on the surface of the earth or inside an aircraft or spacecraft. What we know about quiet high-performance air moving devices and ventilation systems on earth can help us to create systems that perform well in spacecraft. Likewise, what we learn about creating atmospheric revitalization systems for long duration space exploration missions can help us to improve air moving devices and ventilation systems on earth.

Fans are common components in ventilation systems and are critical components in spacecraft atmospheric revitalization systems. In a microgravity environment, air can become stagnant inside a spacecraft without fans. Inside spacecraft fans are required to move the air through the atmospheric revitalization system to maintain the chemical and biological composition of the gases at levels that can sustain human life.

Quiet, efficient fans are also needed in a variety of aircraft propulsion systems. Beginning in 2006, the NASA Glenn Research Center (GRC) Acoustics Branch has been conducting research to examine the aerodynamic and acoustic performance of small fans. A central research question was formed: could the

tools and techniques that had primarily been used to develop quiet and efficient fans for aircraft propulsion systems could be put to broader use to support long duration human exploration missions?

To begin to answer that question, the aerodynamic and acoustic performance of a small fan suitable for cooling electronics was tested in the NASA GRC Acoustical Testing Laboratory (ATL) (Refs. 1, 2, and 3). In 2008, a workshop on small fan aerodynamic and acoustic performance was held at NASA GRC. During this workshop, various perspectives were shared on the challenges of quiet fan performance in spacecraft, in aircraft, and in the information technology industry.

By 2010, research attention at NASA became focused on cabin ventilation fans, historically some of the dominant sources of noise onboard spacecraft. A fan design nominally suited for a spacecraft cabin ventilation system was analyzed by Tweedt in 2010, using a Reynolds-averaged Navier Stokes solver (Ref. 4). Using the same design point conditions for flowrate and pressure rise and overall size constraints, Tweedt designed and analyzed the aerodynamic performance of another axial fan, using best practices in low noise aircraft engine design. A low noise blade-vane count was selected for this design (Ref. 5). Tone noise predictions for this fan were generated by Koch in 2011 (Ref. 6). The aerodynamic design of the axial fan designed by Tweedt in 2010 (Ref. 5) was used to create an additively manufactured thermoplastic prototype fan that was tested in the NASA GRC ATL in 2012 (Ref. 7). In this test, far field noise measurement were recorded as the fan was tested in isolation, without inlet and exhaust ducts and without the ability to throttle the fan through its operating range and to its design point.

This report describes an effort to design, build, and test a metal version of this fan and map its aerodynamic and acoustic performance throughout its operating range. First, details about the metal fan design and manufacture are presented. A test rig used to throttle the fan and to measure the flowrate and pressure rise of the fan was designed, fabricated, and installed in the ATL. The key features of this test rig will be presented, highlighting the fan testing standards that were used. Next, the capabilities of the GRC ATL will be summarized, since all the experiments recorded here were performed inside the ATL. To validate fan tone noise predictions and to gain more detailed acoustic data that could be used to develop quieter fans, a microphone array was constructed and installed in the fan duct and will be described. Finally, a representative sample of the aerodynamic and acoustic results are presented and discussed for the tested fan. While the velocities downstream of the rotor were also measured with a hot wire probe to further validate aerodynamic and acoustic predictions, those results are beyond the scope of this paper. The report concludes with a few recommendations for further research and development of quiet fans for spaceflight.

2.0 Metal Fan Design and Analysis

The spacecraft cabin vent fan prototype was designed to produce 3.64 in. of water pressure rise (907 Pa) at 150 cfm (4.25 m^3/min) of airflow at 12,000 rpm. The metal version of this fan was designed for both traditional machining methods and additive manufacturing methods and features a unique light-weighting casing design. Figure 1 shows the aerodynamic design of the fan rotor, stator, and duct developed by Tweedt (Ref. 5). This aerodynamic design was used in the plastic prototype tested in 2011 shown in Figure 2 and the metal prototype tested in 2021 shown in Figure 3 and Figure 4. The nosecone and the tailcone designs were truncated to minimize the axial length since this fan was intended to be used in a spacecraft with convoluted ductwork. Three hollow aft struts were added to the design for several reasons: a) to provide added structural strength to support the motor since all the fan parts were printed from thermoplastic using stereolithography, a technique that was relatively new to the research team for these purposes at the time, b) to accommodate the motor wiring and the thermocouple that was attached to the motor housing, and c) to ventilate the motor cavity to prevent the motor from overheating. The

honeycomb section in the 2011 plastic fan design that was used as a finger guard and a flow conditioner was omitted from the 2020 metal fan design since the metal fan was installed with long inlet duct.

2.1 Fan Light-Weighting

Efforts were made to reduce the weight of the casing to demonstrate the advantages of additive manufacturing for a flight-ready fan. A stiffening ribbing structure was developed, with a flange on top forming what resembles a T-beam that greatly increases stiffness compared to conventional ribs while reducing weight. The T-beams conform to the periphery of the casing. A cutaway view of the design is shown in Figure 3. The conformal T-beams are oriented on splines that spiral along the axial direction in both directions of the casing with an incidence angle of 45°. The splines repeatedly intersect as they spiral in opposing directions forming a waffle-like pattern. An external view of the design is shown in Figure 4. The design was manufactured and assembled by Trifecta Tool and Engineering, LLC. Direct metal laser sintering (DMLS) using a 3D Systems Laserform printer was used for the non-rotating parts of AlSi12. The rotor was machined of aluminum T6061. The fan weighed 1635.03 g (3.6 lb). Average surface roughness in the hand polished inlet duct was Ra = 1.314 μm (51.732 μin.) and was Ra = 7.235 μm (284.84 μin.) in the unpolished aft duct, as measured by a MAHR Marsurf PS10 profilometer. For comparison, the plastic prototype tested in 2011 (Ref. 6) that was manufactured with stereolithography had an average surface roughness in the inlet duct of Ra = 7.884 μm (310.41 μin.).

2.2 Removable Rotor

One of the significant improvements in the new design is the ability to dismantle the rotor from the motor. The previous design had the rotor permanently cemented on the motor preventing disassembly. This increases the versatility and flexibility of the design, allowing for future modifications and upgrades to be performed. To enable the disassembling of the rotor, a keyless bushing was selected to serve as the interface between the rotor and the motor. The keyless bushing not only friction grips the motor's shaft but also grips on to the rotor, creating a mechanical linkage between the shaft and rotor. To access the tightening mechanism of the keyless bushing from the upstream side of the fan, the nose fairing was made as a separate part that can detach from the rest of the rotor. The rotor assembly is shown in Figure 5 and Figure 6.

2.3 Modal Analysis

A modal analysis was conducted on the rotor using both CREO Simulate and Ansys Mechanical to determine its modal frequencies to ensure that none would be excited under the operating conditions of the fan. The modal analysis was performed under a Free-Free unconstrained boundary condition with the material properties of aluminum T6061.

2.4 Static Structural Analysis

A structural analysis was performed using CREO Simulate. The boundary conditions were a centrifugal force on the blades resulting from them spinning at 12,000 rpm, and a one psi pressure force was applied to the bottom surface of the blades to account for the lift force generated by the fan. The 12,000 rpm value is based on the maximum fan speed that the fan's speed controller is set to allow, and the lift pressure value is a highly conservative estimate based on expected fan performance. The stress levels are shown in Figure 7. The highest stress on the blade occurs at the root of the blades at the junction fillet between the hub of the blisk and the blades. A zoomed-in view of the rotor stress levels is shown in Figure 8. A Campbell diagram is presented in Figure 9.

3.0 Fan Test Description

A test rig was designed and fabricated so that small fans could be throttled through their operating envelopes and the aerodynamic and acoustic measurements could be acquired. The test rig was assembled inside the NASA GRC Acoustical Testing Laboratory (Refs. 8 and 9). The test rig size was constrained slightly by the dimensions of the test chamber, but this is expected to be a very minor effect. Details about the ATL, and the fan test procedure and selected apparatus are given below.

3.1 NASA GRC Acoustical Testing Laboratory

The NASA GRC Acoustical Testing Laboratory was configured as a fully anechoic chamber for this test campaign. The interior dimensions of the ATL are of 7.0- by 5.2- by 5.2-m (23- by 17- by 17-ft). Fiberglass wedges that are 0.86 m (34 in.) deep cover the walls and floor. The wedges are designed to absorb 99 percent of all sound above 100 Hz. Steel grating is mounted over the floor wedges to allow personnel to walk throughout the chamber but still allow sound to pass through to the wedges below. A separate control room is located adjacent to the chamber and was used to house the data acquisition systems and allowed test operators to remotely control the experimental fan safely. The ATL was chosen for this test primarily since far field noise measurements were desired.

3.2 Fan Test Rig Details

The fan test rig was installed on top of the steel grating in the ATL. ISO 5801 (Ref. 10) was largely followed to design the test rig for aerodynamic performance. ASHRAE 68 (Ref. 11) and ISO 5136 (Ref. 12) was used to guide the design and methods for noise testing of a ducted fan. A diagram of the test rig appears in Figure 10. The duct rig was constructed of PVC pipe, though the microphone array, bellmouth, and throttle were fabricated by Protolabs from stereolithography (SLA) material Accura Xtreme White 200 by Vipers, ProJets and/or iPro SLA printers.

3.3 Fan Test Procedure and Selected Apparatus

During the tests, the fan flow rate was set by moving the actuated throttle to the desired position with a Velmex BiSlide linear actuator and controller. Position of the throttle was measured with a TE Connectivity string potentiometer (model TE-SP2-12). Power to the motor was provided by a TDK Lambda 2U Genesys 5 kW DC Power Supply. The motor for the 2021 fan was the same model as the motor for the 2011 fan, a Maxon 48V EC 4 pole brushless DC motor (part number 305015). Fan speed was controlled using a Maxon ESCON Servokontroller (part number 409510) and the fan speed was varied using a dedicated laptop computer running the Maxon motor controller software. Two PCB Piezotronics ICP Accelerometers (part number 325C33) were installed in two places on the fan housing measured vibrations in the vertical and horizontal directions. Temperature of the motor housing was measured with a Type K thermocouple. Current used by the motor to drive the fan was measured with a Phoenix contact universal current transducer (part number MCR-SL_CUC-100-U-2308108). Rig data was recorded with a National Instruments Compact DAQ ethernet chassis (NI cDAQ-9188) and a separate computer running Labview 2020 software.

The contour of the bellmouth was described in ISO 5801. The bellmouth conditioned the flow entering the fan, and a static pressure tap located 25.4 mm (1.0 in.) downstream of the bellmouth curvature was used to calculate and set the flow through the fan during the tests. Location for the static pressure tap on the bellmouth was determined by examining computational fluid dynamics predictions

generated with Solidworks Flow Simulator for the 150 cfm design point condition. Flow rate calculated from the bellmouth static pressure tap was compared with the flow rate calculated from a pitot static tube installed in the inlet duct. The pitot static tube was not installed during the acoustic tests of the fan since it would obstruct the flow and cause unwanted noise.

Sound in the duct upstream and downstream of the fan was measured using a 72-channel microphone array. A recent improvement to in-duct mode measurements (Ref. 13) used a so-called T-array, with an axial line array intersecting a circular ring of sensors. The array used in this test featured 23 microphones in the ring, with a spacing of 12 mm (0.475 in.) between each microphone. Fifty transducers with the same spacing were used for the axial array, with one overlap. Microphone diameter was 4 mm (0.157 in.) The overall axial length of the microphone array was 591 mm (23.275 in.). The resulting performance is that the array can determine a maximum azimuthal mode of order 11 with a frequency of 14,215 Hz, not including convective flow effects. The lower frequency resolution is set by the axial length and is 281 Hz. The lower frequency resolution is set by the axial length and is 281 Hz. Microphone array data was recorded with an HBM Gen3i data acquisition system.

Four external microphones were used to measure noise radiated from the test article. Three microphones were arranged to measure noise radiated from the inlet; one microphone was set-up to measure case radiated noise. The three inlet radiated noise microphones were mounted on poles at a radius of 0.91 m (3.0 ft) from the inlet duct lip. The microphones faces were oriented toward the inlet and placed at angles relative to the duct centerline of –45°, 0, and 45° in the horizontal plane of the duct center line. The microphone measuring the case radiated noise was placed directly above the fan plane, 15.24 cm (6 in.) from the duct. The microphone positions are shown in Figure 9. The microphones were PCB model 378C01 ICP integrated pre-amp which consists of 6.35 mm (0.25 in.) freefield, pre-polarized, 377C01 microphone and 426B03 preamplifier, with programmed Transducer Electronic Data Sheet (TEDS).

Detailed rotor wake velocity measurements were also acquired during this test campaign. Rotor wake velocity measurements can be used to validate aerodynamic and acoustic predictions in more detail. A traversing hot wire probe was inserted into the fan to measure the flow velocity in the wake of the rotor. Fan speed was detected with a Monarch Instruments Remote Optical Laser Sensor (part number 6180-029) upstream of the bellmouth that sensed a piece of reflective tape attached to the rotor hub. The hotwire instrumentation was not installed during acoustic tests or the overall fan aerodynamic performance tests. Results from the hotwire tests will be published later and are beyond the scope of this paper.

4.0 Results

The spacecraft cabin vent fan prototype was designed to produce 3.64 in. of water pressure rise (907 Pa) at 150 cfm (4.25 m^3/min) of airflow at 12,000 rpm. The measured performance was quite close to this, with 3.48 in. of water (867 Pa) at 150.6 cfm (4.26 m^3/min). With the throttle wide open, the observed pressure rise was 0.52 in. of water (130 Pa) and the airflow was 220.4 cfm (6.24 m^3/min). Peak pressure rise was measured as 4.0 in. of water (996 Pa) at 120.7 cfm (3.42 m^3/min). Lower fan speed conditions were also measured. A fan map for three speeds is shown in Figure 11.

A major aspect of the acoustic design of the fan was reducing tone noise by selecting the blade counts such that the first three blade passing tones due to rotor/stator interaction would be generated at azimuthal modes that were cut off due to the size of the duct. This means that the sound would be evanescent and decay quickly rather than propagating through and out of the piping system. The Actran software *cutget* tool was used to compute the cut on frequencies for a 43.85 mm radius (3.45 in. diameter) circular duct with 12 m/s (Mach 0.035) airflow. The results are shown in Table I for frequencies up to 20 kHz. Since the spacecraft cabin vent fan prototype is full-scale, the limits of human hearing are reasonable upper

bounds for the frequency range of interest. The tones generated by the rotor-stator interaction mechanism occur at azimuthal modes *m,* which are governed by the Tyler-Sofrin (Ref. 14) rule,

$$m = nB + kV \tag{1}$$

where for the spacecraft cabin vent fan the blade count $B = 9$ and the vane count $V = 11$. The rotor harmonic, n is a positive integer and the index, k , is an integer. The azimuthal modes, m, are summarized in Table II. The blade passing frequency (BPF) at the fan design speed of 12,000 rpm is 1,800 Hz. The first expected cut-on azimuthal mode is $m = 3$, which occurs at the fourth rotor harmonic ($n = 4$), which is 7,200 Hz at design fan speed of 12,000 rpm. Array microphone 25 is at the intersection of the axial and azimuthal arrays. The sound in the duct is essentially constant down the axial length of the array, so this amounts to a typical example. A single microphone does not identify the modal components of the total sound energy but gives the net amplitude of the unsteady pressure. This is shown in Figure 12 for Reading 31 on 2021-09-02, recorded with the GRC fan. The most evident blade rate tones are BPF at 1,800 Hz and 4xBPF at 7,200 Hz. A non-blade rate tone is evident at the $m = 1$ cut-on frequency of 2,270 Hz. These three tones will be examined in more detail in future reports.

TABLE I.—PREDICTED CUT-ON FREQUENCIES FOR THE FAN

m	Cut-on frequency	*m*	Cut-on frequency
1	2,270	8	11,896
2	3,766	9	13,208
3	5,181	10	14,515
4	6,557	11	15,817
5	7,911	12	17,114
6	9,250	13	18,408
7	10,577	14	19,700

TABLE II.—TYLER-SOFRIN AXIMUTHAL MODES (m) FOR THE FAN CALCULATED FROM EQUATION (1)

nBPF, harmonic of blade passing frequency at 12,000 rpm, Hz	*k* / *n*	*k* = –5	*k* = –4	*k* = –3	*k* = –2	*k* = –1	*k* = 0	*k* = 1
1,800	*n* = 1	–46	–35	–24	–13	–2	9	20
3,600	*n* = 2	–37	–26	–15	–4	7	18	29
5,400	*n* = 3	–28	–17	–6	5	16	27	38
7,200	*n* = 4	–19	–8	**3**	14	25	36	47
9,000	*n* = 5	–10	**1**	12	23	34	45	56
10,800	*n* = 6	**–1**	10	21	32	43	54	65

5.0 Recommendations

Performing this research during the COVID-19 pandemic presented many challenges, which impacted the experiment in different ways. Vibrations measured during the test indicated that further attention to the balance of the rotor, the design of the motor mount, and the alignment of the rotor with the shaft are areas that could be studied further.

6.0 Conclusions

A metal spacecraft cabin ventilation system fan prototype was designed, fabricated, and then tested at the NASA GRC ATL using a duct rig inspired by several standards. The fan was throttled through its operating range, and results indicated that the measured aerodynamic and acoustic performance was in good agreement with predictions. The spacecraft cabin vent fan prototype was designed to produce 3.64 in. of water pressure rise at 150 cfm of airflow at 12,000 rpm. The measured performance was 3.48 in. of water at 150.6 cfm. Using turbofan engine design practices, a low-noise blade-vane count was chosen to try to reduce tone noise generated by this fan by cutting off the first three blade passing frequency tones. In-duct microphone array measurements indicated that the most evident tones occur for frequencies of 1,800 Hz (1 BPF) and 7,200 Hz (4 BPF). A non-blade rate tone is evident at 2270 Hz. These three tones will be examined in more detail in future reports. Further attention to the rotor balance and connections of the motor to the rotor and the stator are recommended. This small fan aerodynamic and acoustic test rig and the NASA GRC ATL are valuable resources available for supporting NASA's aeronautics research and space exploration missions.

References

1. D.E. VanZante, L.D. Koch, M. Wernet, G.G. Podboy, "An Assessment of NASA Glenn's Aeroacoustic Experimental and Predictive Capabilities for Installed Cooling Fans: Part 1: Aerodynamic Performance," NASA/TM—2006-214448, 2006. https://ntrs.nasa.gov
2. L.D. Koch, D.E. VanZante, M. Wernet, G.G. Podboy, "An Assessment of NASA Glenn's Aeroacoustic Experimental and Predictive Capabilities for Installed Cooling Fans; Part 2: Source Identification and Validation," NASA/TM—2006-214450, 2006. https://ntrs.nasa.gov
3. L.D. Koch, D.E. VanZante, "Cool and Quiet Partnering to Enhance the Aerodynamic and Acoustic Performance of Installed Electronics Cooling Fans A White Paper," NASA/TM—2006-214449, 2006. https://ntrs.nasa.gov
4. D.L. Tweedt, "Computational Aerodynamic Simulations of a Spacecraft Cabin Ventilation Fan Design," NASA/CR—2010-216330, 2010. https://ntrs.nasa.gov
5. D.L. Tweedt, "Aerodynamic Design and Computational Analysis of a Spaceflight Vehicle Cabin Ventilation Fan," NASA/CR—2010-216329, 2010. https://ntrs.nasa.gov
6. L.D. Koch, T.D. Shook, D.T. Astler, S.A. Bittinger, "Tone Noise Predictions for a Spacecraft Cabin Ventilation Fan Ingesting Distorted Inflow and the Challenges of Validation," NASA/TM—2012-217681, 2012. https://ntrs.nasa.gov
7. L.D. Koch, C.A. Brown, T.D. Shook, J. Winkel, J.S. Kolacz, D.M. Podboy, R.A. Lo4ew, J.H. Mirecki, "Acoustic Measurements of an Uninstalled Spacecraft Cabin Ventilation Fan Prototype," NASA/TM—2012-217692, 2012. https://ntrs.nasa.gov
8. B.A. Cooper, "NASA Glenn Research Center Acoustical Testing Laboratory," *The Journal of the Acoustical Society of America*, **109(5)**, 2328-2328. 2001.

9. Podboy, D.M., Mirecki, J.H., Walker, B.E., and Sutliff, D.L., "Recent Improvements to the Acoustical Testing Laboratory at the NASA Glenn Research Center," AIAA-2014-072.
10. *Fans—Performance testing using standardized airways*, International Standard ISO 5801:2017(E), (Technical Committee ISO/TC 117, Fans, Geneva, Switzerland, 2017).
11. *Laboratory Method of Testing to Determine the Sound Power in a Duct*, ANSI/ASHRAE 68-1997, (ASHRAE Standard Project Committee 68-1997, TC 2.6, Sound and Vibration Control, Atlanta, Georgia, 1997).
12. *Acoustics-Determination of Sound Power Radiated into a duct by fans and other air moving devices--In-duct method--second edition,* International Standard ISO 5136:2003, (Technical Committee IS/TC 43, Acoustics, Subcommittee SC 1, Noise, Geneva, Switzerland, 2003).
13. D.L. Sutliff, B.E. Walker, "Characteristics Using an Ultrasonic Configurable Fan Artificial Noise Source to Generate Modes-Experimental Measurements and Analytical Predictions," AIAA-2014-2346, 2014. https://doi.org/10.1177/1475472X166308
14. J.M. Tyler, T.G. Sofrin, "Axial Flow Compressor Noise Studies." *S.A.E. Transactions,* 70, 309-332, 1962.

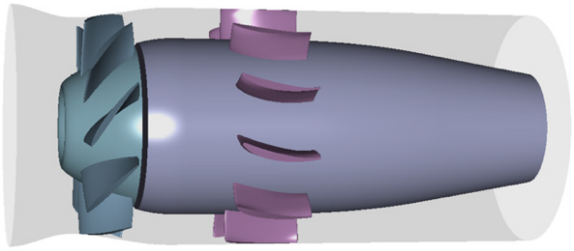

Figure 1.—Fan aerodynamic design of rotor, stator, and duct.

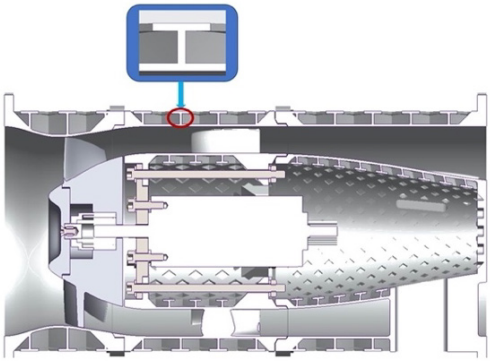

Figure 3.—Cross-section of the metal fan tested in 2021 with T-Beam Stiffening inset.

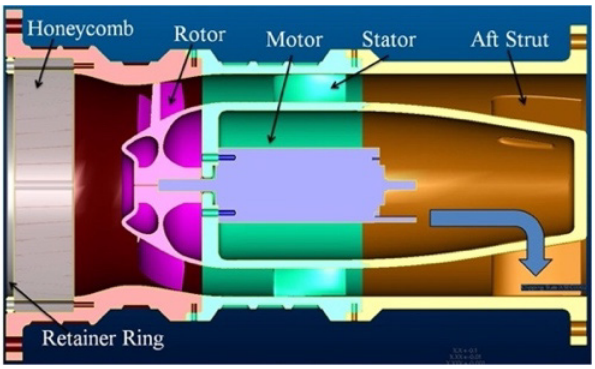

Figure 2.—Cross-section of plastic fan prototype tested in 2011.

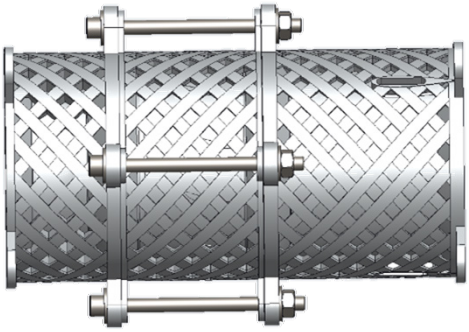

Figure 4.—External view of the metal fan tested in 2021.

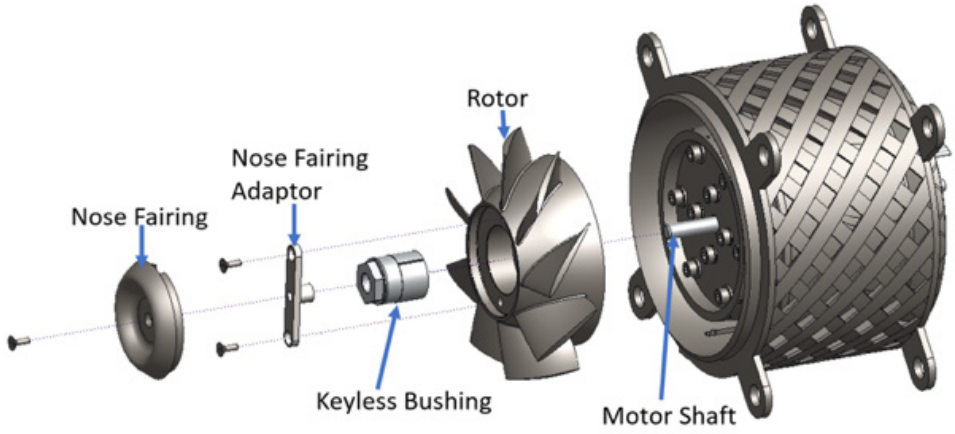

Figure 5.—Exploded view of the rotor assembly.

Figure 6.—Rotor assembly.

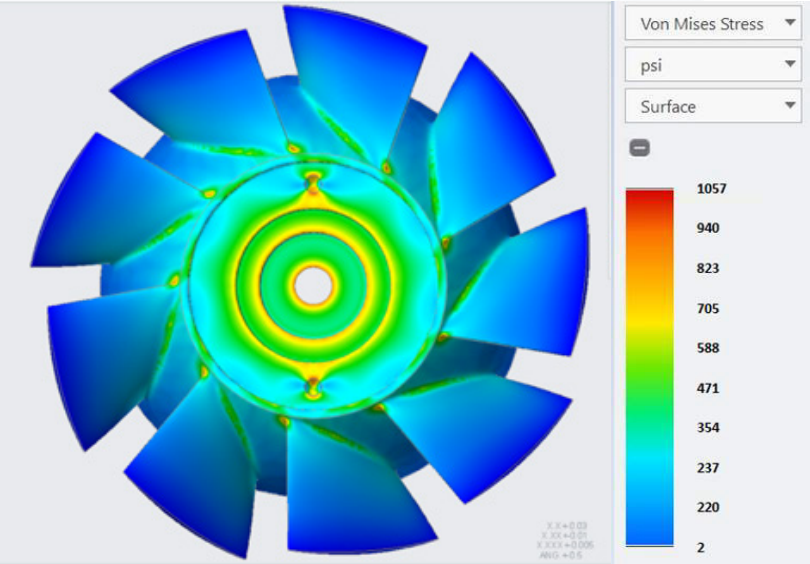

Figure 7.—Rotor stress levels.

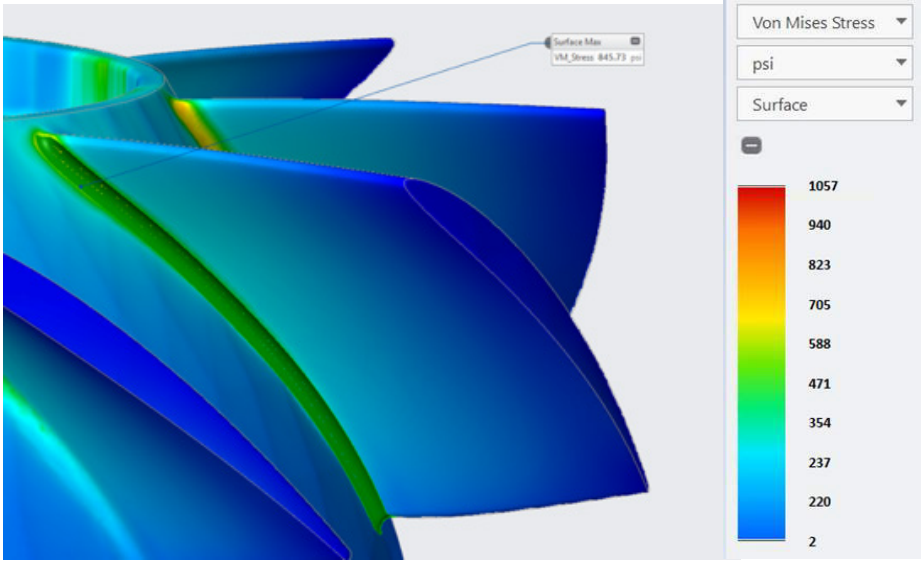

Figure 8.—Rotor blade stress levels.

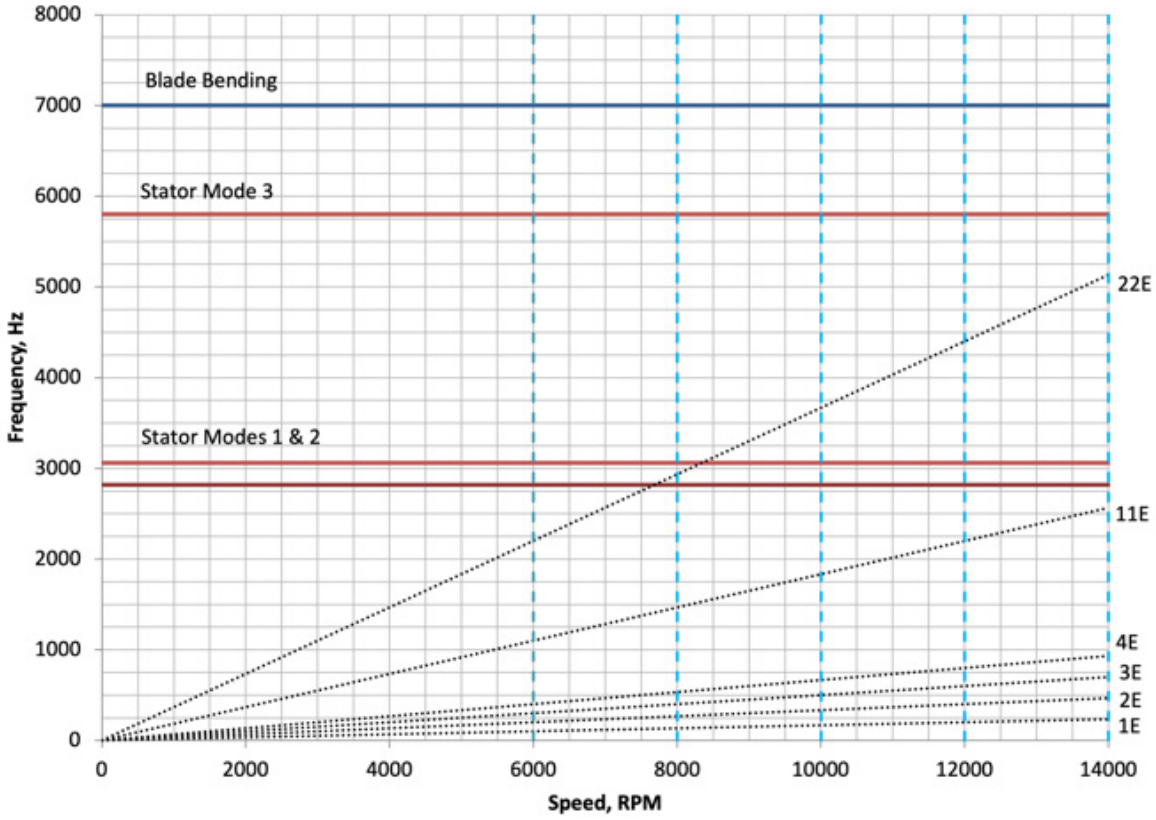

Figure 9.—Campbell diagram.

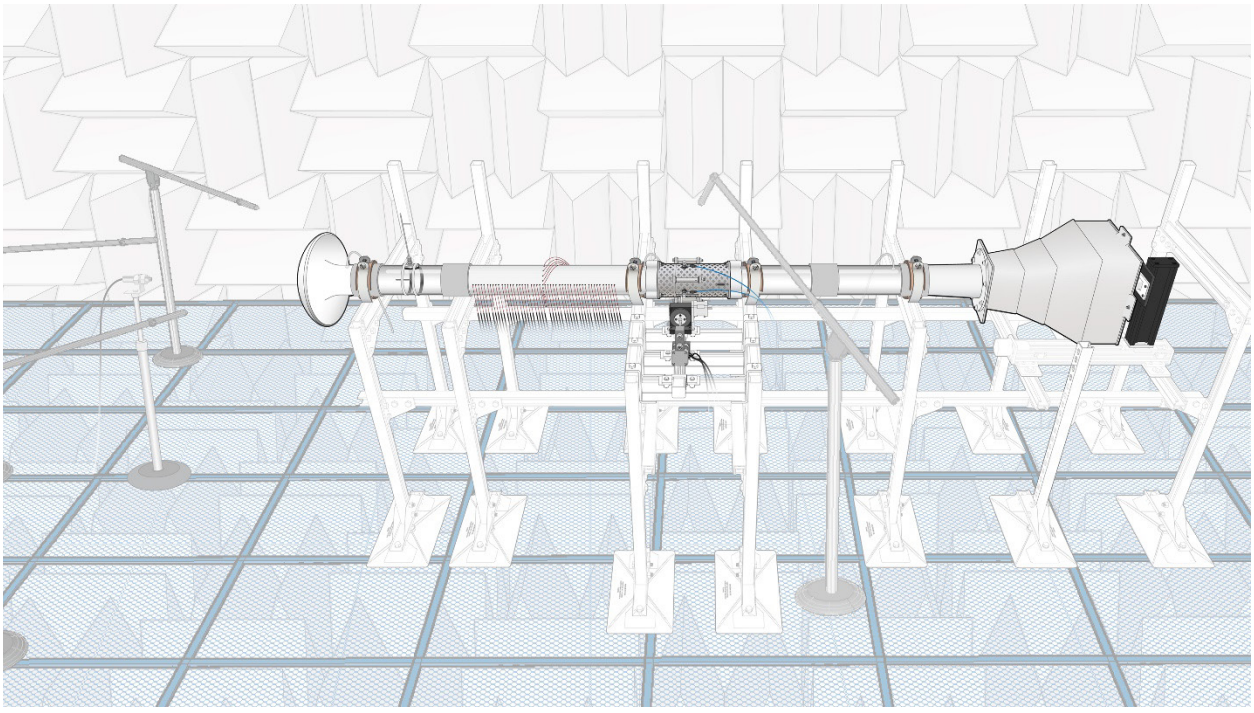

Figure 10.—Illustration of fan test rig installed in the NASA Glenn Acoustical Testing Laboratory, shown with complete set of instrumentation available

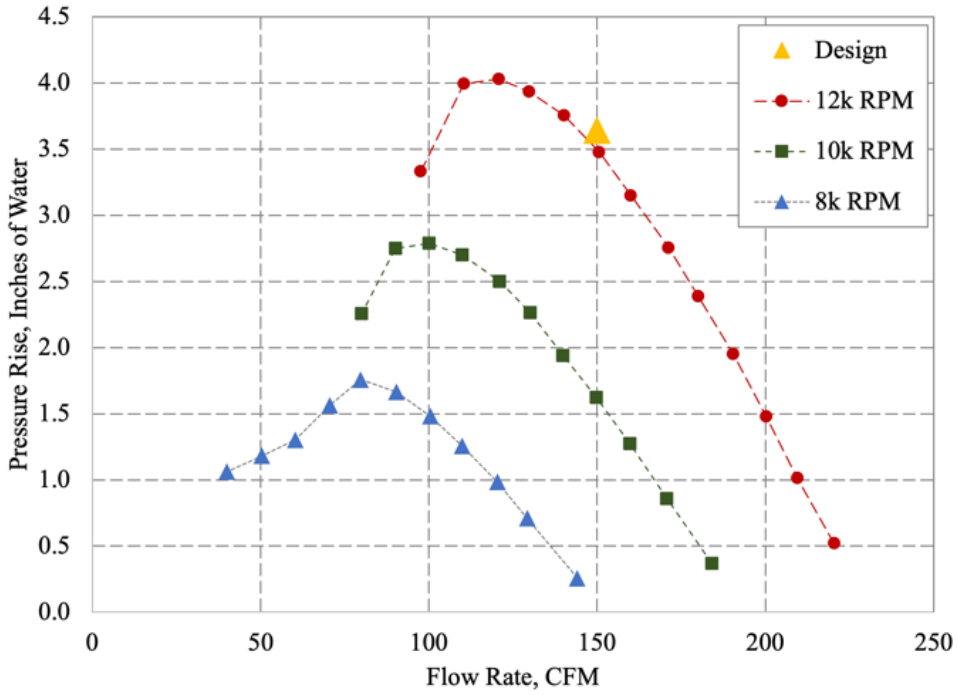

Figure 11.—Fan aerodynamic performance map.

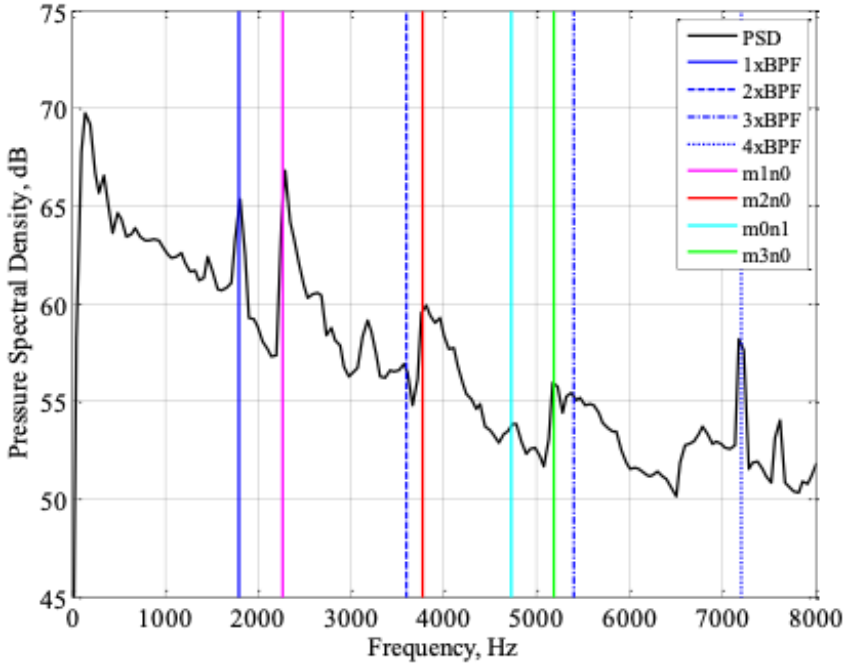

Figure 12.—Spectral density of array microphone 25 annotated with blade rate frequencies and duct mode cut-on frequencies.